COPPER AND SULFUR CO-DOPED ZNO NANOPARTICLES FOR EFFICIENT SOLAR PHOTOCATALYTIC DEGRADATION OF METHYL ORANGE

GIDEY, M.[1] – WELDERFAEL, T.[1] – YADAV, O. P.[2*]

[1] *Chemistry Department, CNCS Aksum University, Aksum, Ethiopia.*

[2] *Chemistry Department, CCS Haryana Agricultural, Hisar, India.*

**Corresponding author*
e-mail: yadavop02[at]yahoo.com

(Received 23rd April 2025; revised 06th July 2025; accepted 15th July 2025)

Abstract. In the present study pure ZnO nanoparticles were prepared using a co-precipitation technique. As-prepared ZnO, was used to prepare Cu-doped ZnO, S-doped ZnO, and Cu & S co-doped ZnO nanostructures by simple hydrothermal method. The synthesized materials were characterized employing XRD, FTIR, and UV-visible spectroscopic techniques. The crystallite particle size of pure ZnO (45.7 nm), was highest among the synthesized powders followed by Cu-doped ZnO (43.29 nm), S-doped ZnO (43.4 nm), and Cu & S co-co-doped ZnO (43.19 nm). The UV-visible absorption spectra of aqueous dispersion of synthesized powders revealed that doping Cu and S in ZnO, both contributed synergistically to lowering of band gap energy from 3.27 eV to 2.35 eV. The photocatalytic efficacies of as-synthesized powders under solar irradiation were determined in terms of methyl orange degradation, as a probe. The observed highest photocatalytic degradation (85 %) of 25 mg L^{-1} dye in aqueous solution within 60 minutes using Cu & S co-doped ZnO load 1.5 gL^{-1} can be attributed to the lower rate of photo-generated charge carriers' recombination as well as lowering of band gap energy enabling absorption of more photons in the visible range of solar radiation. Considering the high photocatalytic efficiency of newly synthesized Cu and S co-doped ZnO powder, the same may be recommended for an effective treatment of methyl orange-contaminated wastewater.
Keywords: *coprecipitation, degradation, nanostructures, photocatalytic, efficiency*

Introduction

Although the mother Earth has so far faced several environmental disasters, yet the worst that has happened during the last 50 years is the contamination of air and water with diverse pollutants imposing serious risk to human health, aquatic life and the entire ecosystem. In the recent years, due to the uncontrolled increasing world population and industrialization, the most serious environmental issue is contamination of water bodies with the stable and non-biodegrade organic and inorganic chemicals such as synthetic dyes, surfactants, fertilizers and heavy metals. The presence of these toxic pollutants in wastewater, originates from industries such as textile, paints, plastics, pharmaceuticals, and agricultural practice (Santhappan et al., 2024). Methyl orange (MO) a member of azo dyes, is widely used in textile, food, paper and cosmetics. However, due to its toxic nature and potential persistence and accumulation, the excessive usage of MO leads to several environmental and health problems. In particular, methyl orange when ingested via food and drinking water can cause irritation to skin and eyes, nausea, vomiting, mental confusion, epilepsy, alzheimer, renal damage, and hypertension (Abdulsalam et al., 2022). Besides these, the dye contaminated water used for irrigation, adversely affects the soil properties, hamper photosynthesis and affect the aquatic biota by disrupting their growth and reproduction (Dutta et al., 2024). Therefore, it is imperative

to eliminate methyl orange dye from contaminated water. Several efforts have been made in the past for regulating the quality of industrial effluents before discharging them into water bodies. But all such attempts for environmental remediation against pollutants proved ineffective because of the high cost of the process involved (Singh et al., 2023). Usually, for treating the dye-contaminated wastewater, processes such as adsorption (Patrón-Prado et al., 2010), electro-coagulation (Getaye et al., 2017), ozonisation (Lanzetta et al., 2023), and chemical and biological methods (Mcyotto et al., 2021; Piaskowski et al., 2018) have been used. However, these techniques have their limitations such as low efficiency, high cost of operation, and generation of solid waste. Adsorption process enables merely phase transference of the contaminant and also generates sludge (Lee et al., 2001). Ozonisation presents a poor stability of ozone affected by salts, pH, and temperature, and the chemical/ biological treatment creates foul smell or is a much slower process.

Heterogeneous photo-catalysis is emerging as an efficient, and environment friendly alternative for the degradation of organic pollutants in aqueous medium (Nazim et al., 2021; Achamo and Yadav, 2016). Transition metal oxides such as TiO_2 and ZnO are generally used for photocatalytic applications including environmental remediation (Gharebaghai et al., 2023; Chen et al., 2020; Kiros et al., 2013; Welderfael et al., 2013). and solar fuel generation (Pezhooli et al., 2022). However, these metal oxides, due to their high band gap energy, are photo responsive only in the UV light to perform photocatalytic reactions (Marschall and Wang, 2014). Moreover, due to the high cost of the UV source, the use of high band gap photocatalysts is not economical for a large scale treatment of wastewater. The low cost ZnO semiconductor with a wide band gap (Eg=3.37 eV), due to oxygen vacancies at its surface can readily generate highly oxidizing H_2O_2 (Xu et al., 2013), therefore, it can improve the mineralization rates of environmental pollutants (Kumar et al., 2023; Jeyapaul et al., 2018; Balcha et al., 2016). Also, ZnO compared to TiO_2, provides larger number of surface active sites with good surface reactivity, therefore, the former can be a more efficient photocatalyst (Gnanaprakasam et al., 2015; Pal and Sharon, 2002). In the present study, pure ZnO, and Cu & S modified ZnO nanostructures have been prepared by precipitation and hydrothermal methods, and the effects of doping Cu and S in ZnO nanoparticles on the degradation of methyl orange in aqueous media under solar radiation, have been studied.

Materials and Methods

Chemicals

Zinc acetate dihydrate [$Zn(CCOO)_2.2H_2O$; 99.9%; MW: 219.50 $g.mol^{-1}$ BLULUX], sodium hydroxide (NaOH 99 %; MW: 40.0 $g.mol^{-1}$, Alpha Chemicals), Oxalic acid dihydrate ($C_2H_2O_4.2H_2O$ MW: 126.065 $g.mol^{-1}$ BDH), copper nitrate trihydrate ($Cu(NO_3)^2.3H_2O$); MW: 241.60 $g.mol^{-1}$ BLULUX], thiourea [$SC(NH_2)_2$; MW: 76.12 $g.mol^{-1}$, BLULUX], ethanol (C_2H_6O, MW: 46.068 g/mol, BLULUX), and methyl orange ($C_{14}H_{14}N_3NaO_3S$, MW: 327.33 $g.mol^{-1}$, Samir Tech. chem). Since the chemicals used in the present study were of high purity and analytical grade, therefore, these were used without any further purification. The molecular structure of methyl orange dye is shown in *Figure 1*.

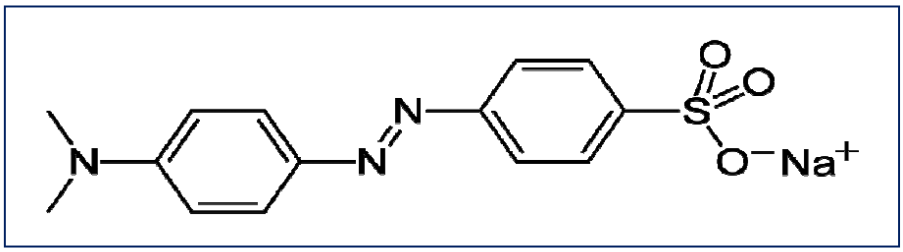

Figure 1. *Molecular structure of methyl orange (MO) dye.*

Preparation of ZnO

Typically, zinc acetate dihydrate (13.2 g) was dissolved in 200 ml of deionized water and the mixture was stirred using magnetic stirrer for 30 min and then 1M NaOH aqueous solution was added, dropwise, with continuous stirring at 60 °C until white precipitates were formed. The precipitates were separated out using Whatman filter paper, washed with deionized water, and ethanol and then dried at 100 °C to get ZnO powder. The product thus obtained was grinded using pestle and mortar and then calcined at 300 °C for 3 hrs before cooling down at the ambient temperature.

Preparation of Cu doped ZnO

Zinc acetate dihydrate (13.2g) and copper nitrate trihydrate (14 g) were separately dissolved in 200 ml each deionized water by magnetic stirring for 30 minutes. The clear solution of copper nitrate trihydrate thus obtained was added slowly into zinc acetate dihydrate aqueous solution with stirring. To the above mixture, 1M NaOH solution was added dropwise until precipitates were formed. The Precipitates were filtered out using Whatman filter paper, and washed repeatedly with deionized water as well as ethanol. The product was dried at 100 °C for an hr and then calcined at 300 °C for 3 hrs to get Cu doped ZnO powder.

Preparation of S-modified ZnO

Zinc acetate dihydrate (13.2 g) and 4.6 g thiourea were dissolved separately in 200 ml each deionized water and magnetically stirred for 30 min. The Zinc acetate dihydrate aqueous solution thus prepared, was added slowly, with continuous stirring, into thiourea solution. To the above mixture, 1M NaOH aqueous solution was added dropwise at 60 °C until precipitates were formed. The precipitates were separated out by filtration and washed with deionized water as well as ethanol and then dried at 100 °C for 1hr. The product obtained was grinded and calcined at 300 °C for 3 hrs followed by grinding at ambient condition to get S-modified ZnO.

Preparation of Cu & S co modified ZnO

Typically, 13.2 g zinc acetate dihydrate was dissolved in 200 mL deionized water. To this copper nitrate trihydrate (14 g) , and thiourea (4.6 g) were added and the mixture was stirred by magnetic stirrer for 30 min. Then 1M NaOH solution was added dropwise, the suspension thus obtained was further stirred at ambient condition for 4 hrs. The precipitates were recovered by filtration using a Whatman paper, washed using deionized water and ethanol. The precipitates were then dried at 100 °C in an oven for 1

hour, grinded to obtain a uniform powder. The product was calcined at 300 °C in a muffle furnace for 3 hrs to get Cu & S co-modified ZnO.

XRD analysis

The crystallite size as well as crystal structure of as-prepared powders were elucidated using an X-ray diffractometer (D8 Advance diffractometer, Bruker, Germany) that provided monochromatic high intensity CuKα radiation (λ=1.5406A0). Each measurement was made at the ambient condition using accelerating voltage 45 kV, and applied current 30 mA operating at the step scan rate 0.0170 degree over 2θ range 50 to 700.

UV visible absorption study

Typically, 10 mg of as-synthesized powder was thoroughly dispersed in 20 ml deionized water and its diffuse absorbance was recorded, over wavelength range 200 nm to 800 nm, using a UV-visible spectrophotometer (Perkin Elmer, SANYO SP65). From the absorption spectra thus obtained, the λ_{max} of the absorption band was evaluated and the band gap energy calculated from $(\alpha h\nu)^2$ versus E(hν) Tau plots.

FTIR study

Typically, a pinch of synthesized powder was thoroughly mixed with a small amount of KBr crystals and paraffin oil. The mixture was then compressed using a hydrolytic press to form a pellet. It was then placed in the path of the IR radiation and scanned over a wavelength range of 4000–400 cm^{-1} at 2 cm^{-1} resolution. The FTIR pattern of synthesized powders was recorded using a Fourier transform infrared spectrometer (JASCO, model 4600).

Photocatalytic degradation study

Using batch operation method, 0.15 g as-synthesized powder was added to 100 ml of 25 mg L^{-1} aqueous solution of methyl orange taken in a 400 ml reactor tube made of Pyrex glass (*Figure 2*). The reaction mixture was magnetically stirred under dark for 30 min to reach a sorption/desorption equilibrium before irradiating the dye aqueous solution under solar radiation during 11 AM to 2 PM on clear days at Chemistry Department of Aksum University (14.10630 N, 38.70790 E). Five ml each of the reaction mixture was collected at regular intervals, and centrifuged at 3000 rpm for 15 min. Absorbance of the clear supernatant liquid was recorded at 460 nm using a double-beam UV-visible spectrophotometer (Carry 60). Percentage degradation of methyl orange dye was calculated using the Eq. (1):

$$\%\ degradation = \frac{A0-At}{A0} X100 \qquad \text{Eq. (1)}$$

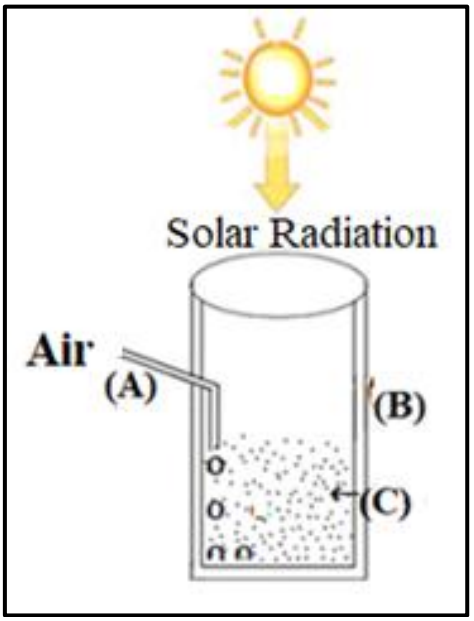

Figure 2. *The arrangement of batch operation photocatalytic Reactor: (A) inlet tube for air purging, (B) 500 ml size pyrex glass beaker and (C) the reaction mixture.*

Where, A_0 & A_t are absorbance values at the initial stage of irradiation and at the reaction time t, respectively.

Results and Discussion

XRD analysis

The XRD patterns of synthesized pure ZnO, Cu doped ZnO, S-doped ZnO and Cu & S co-doped ZnO powders are shown in *Figure 3*. The diffraction peaks appearing at 2θ: 31.7º, 34.4º, 36.2º, 47.52º, 56.5º, 62.88º, and 67.9º assigned to crystal planes (1 0 0), (002), (101), (102), (110), (103) and (200), respectively, reveal the hexagonal wurtzite crystal structure of ZnO, in agreement with the JCPDS No: 361451. The observed similar XRD pattern for pure ZnO as well as Cu-doped ZnO powders, indicates that doped Cu atom fits well at the vacant Zn lattice site of ZnO. The appearance of additional diffraction peaks at 2θ=24.78° and 28.5°in the XRD spectra of S-doped ZnO, may be due to the diffractions from orthorhombic S8 crystal planes. However, these additional peaks disappear in the XRD spectra of Cu & S doped ZnO may be due to the interaction of doped Cu and S resulting in the disruption of S8 crystal phase. The average crystalline size of synthesized powder was obtained using the DebyeScherer formula (Scherrer, 1918):

$$D = \frac{k\lambda}{\beta cos\theta} \qquad \text{Eq. (2)}$$

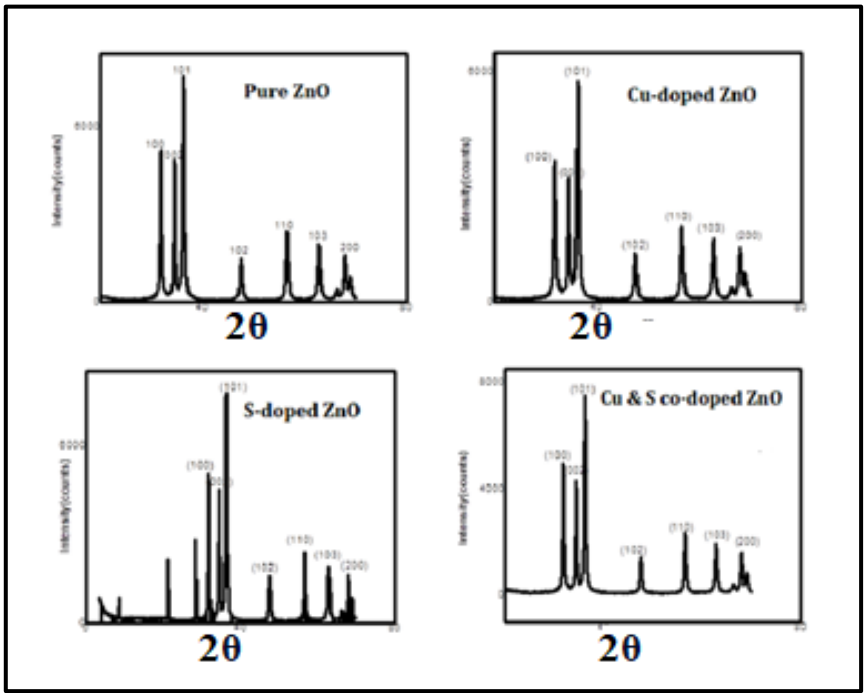

Figure 3. *XRD patterns of as-synthesized pure ZnO, Cu-doped ZnO, S-doped ZnO, and Cu & S co-doped ZnO powders.*

Where, D is the particle size in nanometer, ʎ is the wavelength (0.15406 nm) for CuKα radiation used, k is a constant (0.94), β is full width at half maxima (FWHM) of the most intense diffraction peak from (101) crystal plane in the XRD spectrum, and θ is the Bragg's angle. The calculated crystalline size for the studies powders along with β, and diffraction peak position (2θ) for the studied powders are given in *Table 1*. The particle size of pure ZnO (45.7 nm) decreases to 43.3 nm upon doping copper which may be because of smaller size Cu^{+2} ions (71 pm) replacing larger Zn^{+2} (radius 74 pm) in the crystal lattice sites of ZnO. The average crystallite size of S-doped ZnO (43.4 nm) is also smaller compared to that of undoped ZnO due to retarding effect of doped sulfur causing strain in the ZnO crystal (Sun et al., 2010). The lowest crystallite size (43.2 nm) of Cu & S co-doped powder may be due to the cumulative effects of above described lower Cu size than Zn, and the crystal growth retardation by Sulfur (*Figure 3*).

Table 1*. Diffraction angle (2Θ), β, and average crystallite size (D) for synthesized powders from Debye Scherer equation.*

Sample	2Θ (Degree)	β (radians)	D (nm)
Pure ZnO	36.23	0.04241	45.7
Cu-doped ZnO	36.27	0.04450	43.3
S-doped ZnO	36.25	0.04415	43.4
Cu & S co-doped ZnO	36.21	0.04410	43.2

FTIR study

FTIR spectra of synthesized pure ZnO, S-doped ZnO, Cu-doped ZnO and Cu & S co-doped ZnO powders, scanned over the frequency range: 400-4000cm^{-1}, are shown in *Figure 4*. The absorption bands appearing in spectra within 400 -500 cm^{-1} are ascribed to Zn-O stretching vibration in the wurtzite structure of ZnO. A broad peak within 3300-3500cm^{-1}, and around 1500-1600 cm^{-1} are assigned to stretching and

bending vibration modes, respectively, for water molecules adsorbed at powders from the environment. The observed absorption peaks within 2000-2200cm^{-1} and at 2900cm^{-1} are attributed to the stretching vibrational modes of C=O of adsorbed CO_2 on the photocatalysts powders.

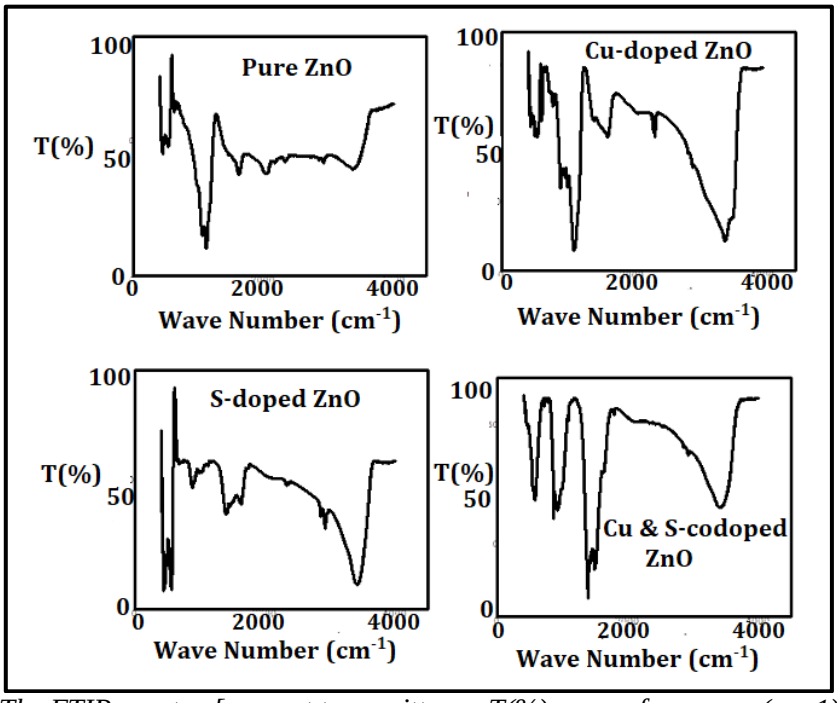

Figure 4. *The FTIR spectra [percent transmittance T(%) versus frequency (cm-1) plots] for synthesized pure ZnO, Cu-doped ZnO, S-doped ZnO, and Cu & S co-doped ZnO powders.*

Determination of band gap energy

The band gap energy of as-synthesized semiconductor photocatalyst powders were determined from their UV-Visible absorption data employing the Tau plot method. This method involves plotting $(\alpha h\nu)^{1/n}$ versus hν, where α is the absorption coefficient, hν is the photon energy, and n is a parameter also called power factor that depends on the type of electronic transition. The power factor (n) is chosen based on the type of electronic transition: 0.5 for allowed direct, 2 for allowed indirect, 1.5 for forbidden direct, and 3 for forbidden indirect transitions. In the present case n=0.5. The absorption wavelength (ʎ) in nm, was converted to photon energy (hv) using Eq. (3):

$$hv = 1240/ʎ \qquad \text{Eq. (3)}$$

Absorption coefficient (α) was calculated from the absorbance (A), and the sample thickness (t) using Eq (4):

$$\alpha = 2.303A/t \qquad \text{Eq. (4)}$$

For a crystalline semiconductor such as ZnO, the band gap energy (E_g) and optical absorption coefficient (α) are related by Eq. (5):

$$(\alpha h\nu)^2 = A(h\nu - E_g) \qquad \text{Eq. (5)}$$

eISSN: 2716-6341
https://doi.org/10.55197/qjoest.v6i3.236

Where, α, hν, Eg and A represent the optical absorption coefficient, photon energy, band gap energy and proportionality constant, respectively. The Tau plots, (αhν)2 versus E(hν), for pure ZnO, Cu-doped ZnO, S-doped ZnO, and Cu & S co-doped ZnO powders are shown in *Figure 5*. A tangent drawn on the curve of the Tau plot intersecting to zero absorption coefficient (i.e. where, αhν)2=0) gives the band gap energy (Eg) in electron volt (eV). The band gap energy (Eg) thus obtained for pure ZnO, Cu-doped ZnO, S-doped ZnO and Cu & S co-doped were: 3.2, 2.9, 2.8 and 2.6 eV, respectively, indicating that the effective band gap energy (Eg) of ZnO decreases upon doping both Cu as well as S.

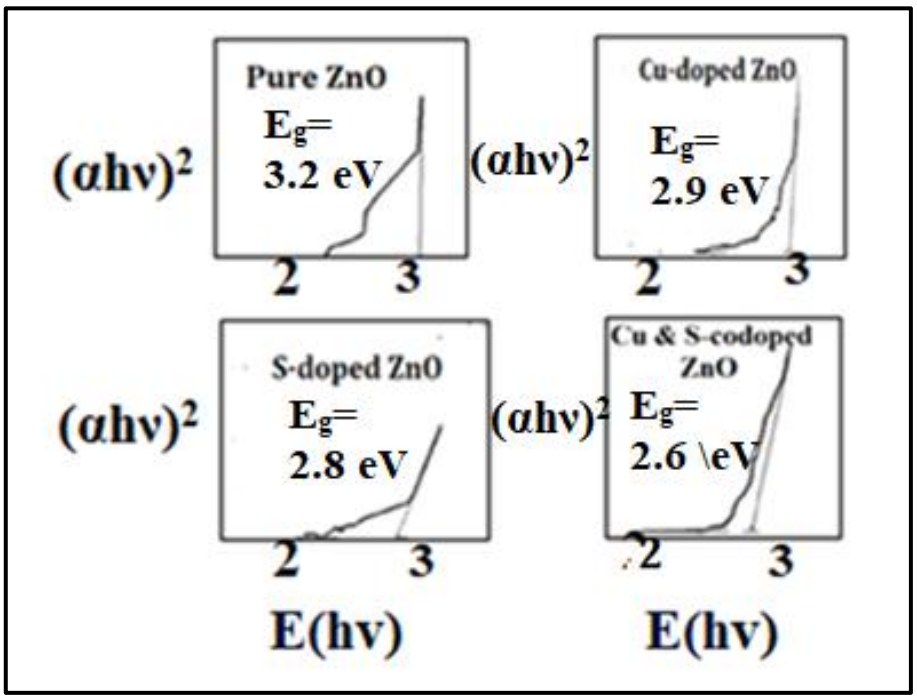

Figure 5. *Tau plots, (αhν)2 versus E(hν), and the derived band gap energy (Eg) of as-synthesized photocatalyst powders: Pure ZnO (3.2eV), Cu-doped ZnO (2.9 eV), S-doped ZnO (2.8 eV), and Cu & S co-doped ZnO (2.6 eV).*

Photocataltytic activity

Photocatalytic activities of synthesized powders were studied following the degradation of methyl orange (MO) range dye in its aqueous solution under solar radiation, as a probe. Percent degradation of MO under solar radiation as a function of reaction time using as-synthesized pure ZnO, Cu-doped ZnO, S-doped ZnO, and Cu & S co-doped ZnO powders as catalyst, are presented in Table 2, and their corresponding plots are shown in Figure 6. Photocatalytic degradation of MO dye at 1 hr with MO initial concentration 25 mg L^{-1}, and catalyst load: 8 gL^{-1}, was highest (85.0 %) using Cu & S co-doped ZnO, followed by S-doped ZnO (82.2%), Cu-doped ZnO (79.1%) and Pure ZnO (75.0%). Higher catalytic activity of Cu-doped ZnO, compared to Pure ZnO, could be due to the diminished rate of charge carriers recombination owing to the electron-trapping by doped copper at the conduction band of the semiconductor. The doped Cu in ZnO also creates localized energy level due to its 3d π-orbitals enabling the

narrowing of effective band gap thus harvesting more photons in the visible radiation. Higher activity of S-doped ZnO compared to pure ZnO could be attributed to creation of additional energy level between conduction and valence bands by 3p π-orbitals of doped sulfur thereby shifting of the absorption edge in visible region of solar radiation thus harvesting more photons. The observed highest photocatalytic activity of Cu & S co-doped ZnO may be due to synergetic effect of electron trapping by copper doping and band gap narrowing by Sulfur doping. The observed high catalytic activity of synthesized Cu & S co-doped ZnO infers that this new material can be effectively employed for treating wastewater contaminated with methyl orange dye pollutant.

***Table 2**. Percent degradation of methyl orange dye at different reaction times using as-synthesized pure ZnO, Cu-doped ZnO, S-doped ZnO and Cu & S co-doped ZnO powders as catalysts (MO initial concentration 25 mg L^{-1}, and catalyst load: 1.5 gL^{-1}).*

Time (min)	% Degradation (Pure ZnO)	% Degradation (Cu-doped ZnO)	% Degradation (S-doped ZnO)	% Degradation Cu & S co-doped ZnO
0	0	0	0	0
10	34.4	45.3	53.6	59.5
20	53.3	59.2	63.2	70.7
40	66.7	69.0	73.8	79.5
60	75.0	79.1	82.2	85.0

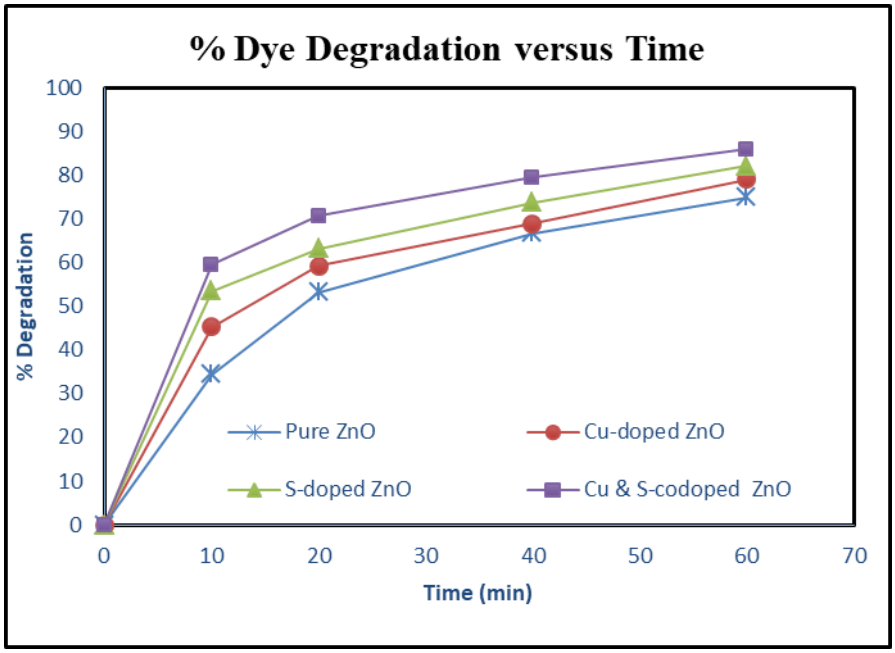

***Figure 6.** Plots of % degradation of methyl orange (MO) dye as a function of reaction time (min) using as-synthesized photocatalyst powders: Pure ZnO, Cu-doped ZnO, S-doped ZnO, and Cu & S co-doped ZnO (MO dye initial concentration 25 mgL^{-1}; catalyst load: 1.5 gL^{-1}).*

Mechanism of dye degradation

A proposed mechanism of photocatalytic degradation of methyl orange (MO) dye using Cu & S co-doped ZnO nanoparticles is described as below. Upon exposing to the sunlight, ZnO absorbs a photon of suitable energy to promote an electron (e^-) from the valence band (VB) to the conduction band (CB), leaving behind a positively charged hole (h^+) at the VB according to Eq. (6). The photoexcited electron (e^-_{CB}) either recombines with the hole (h+) or it combines with a surface adsorbed O_2 molecule forming an anionic oxygen molecule radical ($\bullet O_2^-$) as per Eq. (7). The radical ($\bullet O_2^-$)

further reacts with hydrogen ions from water molecule forming hydroxide •OH radical according to equation (8). The •OH radical oxidizes a molecule of MO forming non-toxic degradation products such as H_2O, CO_2, as indicated in Eq. (9). The hole at the VB (h^+_{VB}) can also directly degrade a MO molecule as shown in Eq. (10).

$ZnO) + h\nu \rightarrow e^-_{CB} + h^+_{VB}$ Eq. (6)

$e^-_{CB} + O_2 \rightarrow {}^{\bullet}O_2^-$ Eq. (7)

${}^{\bullet}O_2^- + 2H^+ \rightarrow 2{}^{\bullet}OH$ Eq. (8)

${}^{\bullet}OH + MO \rightarrow CO_2 + H_2O$ Eq. (9)

$h^+_{VB} + MO \rightarrow H_2O + CO_2\uparrow + etc.$ Eq. (10)

The doped Cu in ZnO, besides trapping the photo-excited electrons, also creates localized energy level due to its 3d π-orbitals thus minimizing charge carriers recombination and harvesting more photons in the visible radiation. The doped sulfur also creates new energy levels between VB and CB due to its 3p π-orbitals promoting more absorption of visible light photons resulting in improved degradation of dye molecules. Therefore, co-doping of Cu and S in ZnO exhibits synergistic effect towards enhancing the photocatalytic degradation of MO. The schematic of photocatalytic degradation of methyl orange dye using as-synthesized Cu & S co-doped ZnO powder is shown in *Figure 7*.

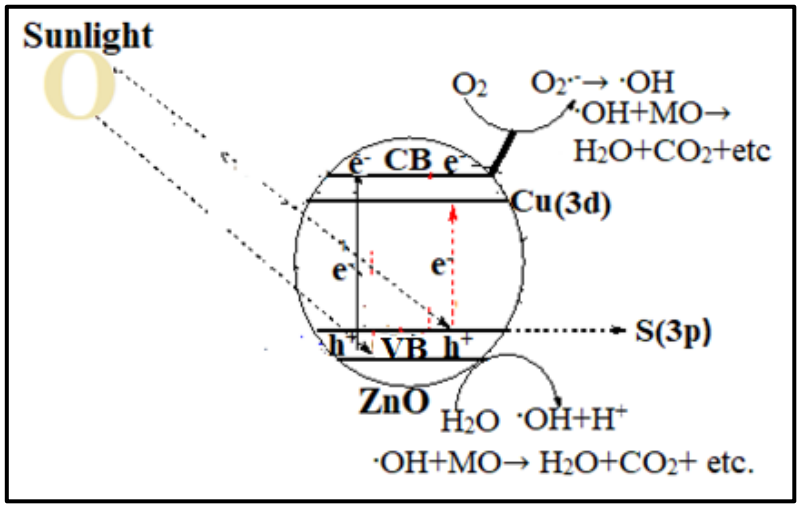

Figure 7. *Mechanism of photocatalytic degradation of methyl orange (MO) dye using as-synthesized Cu & S co-doped ZnO photocatalyst powder (CB=conduction band; VB=valence band; Cu(3d)=Energy level due to doped Cu; S(3p)=Energy level due to doped S).*

Conclusion

Pure ZnO, Cu-doped ZnO, S-doped ZnO, and Cu & S codoped ZnO nanoparticles were synthesized by simple co-precipitation method and characterized using XRD, UV-Visible and FTIR techniques. The XRD analysis of synthesized undoped as well as doped ZnO powders revealed their hexagonal wurtzite structure. UV-visible absorption

study enabled the evaluation of band gap energies of the synthesized photocatalyst powders. The Cu & S-co-modified ZnO powder exhibited highest (85 %) degradation of methyl orange dye within one hour, followed by S-doped ZnO, Cu-doped ZnO and Pure ZnO. The copper & sulfur co-doping in ZnO synergistically improved the degradation of dye by minimizing charge carriers' recombination and narrowing the band gap energy. As the newly synthesized Cu & S co-doped ZnO has exhibited high catalytic activity in degrading the studied dye, therefore, it can be used for an effective treatment of wastewater contaminated with methyl orange dye as pollutant.

Acknowledgement

The authors are grateful to Aksum University, Adigrat pharmaceutical Factory (APF), and Addis Ababa University for providing access to different experimental facilities.

Conflict of interest

The authors confirm that there is no conflict of interest involve with any parties in this research study.

REFERENCES

[1] Abdulsalam, K.A., Olagoke, H.B., Oladosu, I.A., Olawoye, B.M., Amodu, B.H., Fako-rede, O.K., Tiamiyu, A., Owolabi, S.O. (2022): Methyl Orange, An Organic Dye: Its Health Impact And Sorptive Removal From Waste Water. – International Journal of Progressive Sciences and Technologies (IJPSAT) 33(1): 150-160.

[2] Achamo, T., Yadav, O.P. (2016): Removal of 4-Nitrophenol from Water Using Ag-NP-Tridoped TiO2 by Photocatalytic Oxidation Technique Ubertas Academica. – An AlyticAl Chemistry Insights 11: 29-34.

[3] Balcha, A., Yadav, O.P., Dey, T. (2016): Photocatalytic degradation of methylene blue dye by zinc oxide nanoparticles obtained from precipitation and sol-gel methods. – Environmental Science and Pollution Research 23(24): 25485-25493.

[4] Chen, D., Cheng, Y., Zhou, N., Chen, P., Wang, Y., Li, K., Huo, S., Cheng, P., Peng, P., Zhang, R., Wang, L. (2020): Photocatalytic degradation of organic pollutants using TiO2-based photocatalysts: A review. – Journal of Cleaner Production 268: 14p.

[5] Dutta, S., Adhikary, S., Bhattacharya, S., Roy, D., Chatterjee, S., Chakraborty, A., Banerjee, D., Ganguly, A., Nanda, S., Rajak, P. (2024): Contamination of textile dyes in aquatic environment: Adverse impacts on aquatic ecosystem and human health, and its management using bioremediation. – Journal of Environmental Management 353: 22p.

[6] Getaye, M., Hagos, S., Alemu, Y., Tamene, Z., Yadav, O.P. (2017): Removal of malachite green from contaminated water using electro-coagulation technique. – Journal of Analytical & Pharmaceutical Research 6(4): 4p.

[7] Gharebaghai, A., Magham, A.H.J., Hokmabadi, L. (2023): Photocatalytic-Degradation of Some Organic Pollutants in Water by ZnO Nanoparticles Synthesized by a Simple Green Method. – Russian Journal of Physical Chemistry A 97(14): 3212-3218.

[8] Gnanaprakasam, A., Sivakumar, V.M., Sivayogavalli, P.L., Thirumarimurugan, M. (2015): Characterization of TiO2 and ZnO nanoparticles and their applications in photocatalytic degradation of azodyes. – Ecotoxicology and Environmental Safety 121: 121-125.

[9] Jeyapaul, T., Harikengaram, S., Chellamani, A. (2018): An Efficient and Enhanced Photocatalytic Activity of ZnO Nanoparticles on Mineralization of Congo Red Dye in Aqueous Medium. – International Journal of Engineering Science Invention 7(3): 12-18.
[10] Kiros, G., Yadav, O.P., Tadesse, A. (2013): Effect of Ag-N co-doping in nanosize TiO2 on photo-catalytic degradation of methyl orange Dye. – Journal of Surface Science and Technology 29: 1-14.
[11] Kumar, G., Mukherjee, I., Dubey, M., Vellenki, B.P., Dutta, R.K. (2023): Photocatalytic degradation of tetracycline in aqueous medium using ZnWO4/Bi2MoO6 nanocomposites under natural sunlight. – International Journal of Environmental Science and Technology 20(3): 2903-2918.
[12] Lanzetta, A., Papirio, S., Oliva, A., Cesaro, A., Pucci, L., Capasso, E.M., Esposito, G., Pirozzi, F. (2023): Ozonation processes for color removal from urban and leather tanning wastewater. – Water 15(13): 13p.
[13] Lee, J.K., Gu, J.H., Kim, M.R., Chun, H.S. (2001): Incineration characteristics of dye sludge in a fluidized bed incinerator. – Journal of Chemical Engineering of Japan 34(2): 171-175.
[14] Marschall, R., Wang, L. (2014): Non-metal doping of transition metal oxides for visible-light photocatalysis. – Catalysis Today 225: 111-135.
[15] Mcyotto, F., Wei, Q., Macharia, D.K., Huang, M., Shen, C., Chow, C.W. (2021): Effect of dye structure on color removal efficiency by coagulation. – Chemical Engineering Journal 405: 13p.
[16] Nazim, M., Khan, A.A.P., Asiri, A.M., Kim, J.H. (2021): Exploring rapid photocatalytic degradation of organic pollutants with porous CuO nanosheets: synthesis, dye removal, and kinetic studies at room temperature. – ACS Omega 6(4): 2601-2612.
[17] Pal, B., Sharon, M. (2002): Enhanced photocatalytic activity of highly porous ZnO thin films prepared by sol–gel process. – Materials Chemistry and Physics 76(1): 82-87.
[18] Patrón-Prado, M., Acosta-Vargas, B., Serviere-Zaragoza, E., Méndez-Rodríguez, L.C. (2010): Copper and cadmium biosorption by dried seaweed Sargassum sinicola in saline wastewater. – Water, Air, & Soil Pollution 210(1): 197-202.
[19] Pezhooli, N., Rahimi, J., Hasti, F., Maleki, A. (2022): Synthesis and evaluation of composite TiO2@ ZnO quantum dots on hybrid nanostructure perovskite solar cell. – Scientific Reports 12(1): 9p. Piaskowski, K., Świderska-Dąbrowska, R., Zarzycki, P.K. (2018): Dye removal from water and wastewater using various physical, chemical, and biological processes. – Journal of AOAC International 101(5): 1371-1384.
[20] Santhappan, J.S., Kalaiselvan, N., Assis, S.M., Amjith, L.R., Glivin, G., Mathimani, T. (2024): Origin, types, and contribution of emerging pollutants to environmental degradation and their remediation by physical and chemical techniques. – Environmental Research 257: 12p.
[21] Scherrer, P. (1918): Göttinger nachrichten math. – Phys 2: 98-100.
[22] Singh, B.J., Chakraborty, A., Sehgal, R. (2023): A systematic review of industrial wastewater management: Evaluating challenges and enablers. – Journal of Environmental Management 348: 34p.
[23] Sun, Y., He, T., Guo, H., Zhang, T., Wang, W., Dai, Z. (2010): Structural and optical properties of the S-doped ZnO particles synthesized by hydrothermal method. – Applied Surface Science 257(3): 1125-1128.
[24] Welderfael, T., Yadav, O.P., Taddesse, A.M., Kaushal, J. (2013): Synthesis, characterization and photocatalytic activities of Ag-N-codoped ZnO nanoparticles for degradation of methyl red. – Bulletin of the Chemical Society of Ethiopia 27(2): 221-232.
[25] Xu, X., Chen, D., Yi, Z., Jiang, M., Wang, L., Zhou, Z., Fan, X., Wang, Y., Hui, D. (2013): Antimicrobial mechanism based on H2O2 generation at oxygen vacancies in ZnO crystals. – Langmuir 29(18): 5573-5580.